

PACS numbers: 42.25.Fx; 87.64.Cc
DOI: 10.1070/QE2008v038n06ABEH013941

Ray-wave approximation for calculating laser radiation scattering by a transparent dielectric spheroidal particle

A.E. Lugovtsov, S.Yu. Nikitin, A.V. Priezzhev

***Abstract*. A theoretical model is developed and an algorithm is proposed for calculating far-field light scattering by a transparent dielectric particle significantly larger than a wavelength. The accuracy of this algorithm is close to that of the discrete dipole approximation. The calculation time for this algorithm in the case of particles with the size parameter higher than 50 is much lower than that for the discrete dipole approximation. Scattering diagrams for spheroidal particles of different sizes, orientations and refractive indices are calculated. The proposed algorithm has a great potential for quick calculations of parameters of light scattering by large biological particles such as erythrocytes and their aggregates, bacteria, etc.**

Keywords: *light scattering, spheroidal particles, geometric optics approximation, ray-wave approximation, discrete dipole approximation, erythrocytes.*

1. Introduction

A spheroid (ellipsoid of rotation) is the simplest model of a particle for which the light scattering depends on its spatial orientation. Spheroids are more adequate models of numerous biological particles, in particular erythrocytes and their linear aggregates, than spheres [1]. A normal erythrocyte can be modeled by an oblate spheroid, while an erythrocyte deformed in the shear flow or an aggregate of erythrocytes such as a rouleaux – by a prolate spheroid [2]. The correct choice of a light scattering phase function of both a single erythrocyte and a cell aggregate and of other spheroidal particles is important for modeling light propagation in blood and blood-containing tissues [1, 3]. This is also important for the interpretation of measurement data obtained with flow cytometers [4], laser Doppler velocimeters and particle sizers [5], in particular at their application to the study of blood-cell and liquid-droplet suspensions (sprays).

The general analytic solution of the problem of a plane electromagnetic wave scattered by an arbitrary spheroid is known [6, 7]. This solution can be regarded as a generalisation of the Mie theory on the case of a spheroid. The T-matrix method ([8], Chapter 6) yields precise solutions of the problem of light scattering by any nonspherical particles, in particular by spheroids. However, these solutions are quite cumbersome. Thus a number of authors have considered the problem of light scattering by a spheroid in various approximations. In particular, in papers [9 – 11] a simpler analytic solution is proposed describing the light scattering in the approximation of a highly elongated spheroid with the relative refractive index $n > 1.2$. In paper [12], the appropriateness of the distribution of the phase function extremuma is analysed for a particular case of a uniform spheroid, whose rotation axis coincides with the direction of the incident wave, and the relative refractive index $1.025 < n < 1.200$. Investigation is performed within the framework of Wentzel – Kramers – Brillouin, Rayleigh – Gans – Debye, Fraunhofer and anomalous diffraction approximations [2]. The equation in generalised coordinates is obtained, which relates the extremuma location to the parameters of the spheroid. In papers [13, 14], the diffraction on, reflection from and transmission through an arbitrarily oriented spheroid of various components of polarised light are calculated within the framework of the ray optics approximation. Cross-polarisation effects are found that are manifested by the rotation of the polarisation plane of the scattered waves. Calculations of the phase function for $n = 1.333$ are presented. In papers [15, 16], the phase functions and integral cross sections of light scattered by spheroids are calculated in the Rayleigh – Gans – Debye approximation. The analysis is performed by means of the field expansion into a three-dimensional spatial spectrum. In paper [17], the effect of nonsphericity and the relative refractive index on the angles, corresponding to the maxima of the scattering intensity (angles of a rainbow) is studied.

A number of modern numerical techniques such as discrete-dipole approximation (DDA) and finite difference time domain method (FDTM) allow solving the problem of light scattering by arbitrary nonspherical particles, including spheroids, with a high precision [8, 18]. However, the laboriousness of these calculations highly depends on the size parameter $2\pi nd/\lambda$ (d is the characteristic size of the particle and λ is the light wavelength). In partucular, when implemented on a contemporary personal computer, the DDA method requires significant time expenditures to calculate the light scattering by optically soft spheroids with size parameters higher than 100 or by smaller spheroids with $n > 1.5$. That is why the search for approximate methods of a sufficiently precise and fast solution of the

A.E. Lugovtsov, S.Yu. Nikitin, A.V. Priezzhev Department of Physics, M.V. Lomonosov Moscow State University, Vorob'evy Gory, 119992 Moscow, Russia; e-mail: avp2@mail.ru, anlug@tut.by

Received 12 March 2008
Kvantovaya Elektronika **38** (6) 606 – 611 (2008)
Translated by A.E. Lugovtsov

problem that does not require significant computational resources still remains urgent. One of such methods is considered in this paper. The fastness of calculations of light scattering by particles is necessary if the parameters of these particles quickly change in time by this or that reason (for instance, in the case of biological particles affected by external factors).

2. Methods

Consider a transparent homogeneous spheroidal particle with the refractive index n_2, surrounded by a medium with the refractive index n_1 (Fig. 1). The particle is illuminated by a plane monochromatic light wave at the wavelength λ. We need to calculate the angular distribution of the intensity of light scattered by the particle. We will neglect the absorption of light by the particle as well as by the surrounding medium, which is true for biological tissues in the wavelength range from 600 to 1000 nm (the so-called 'transparency window'). Our model of the light wave as a wave with ideal temporal and spatial coherence is applicable if the coherence length and coherence radius of the incident laser beam exceed well the particle size.

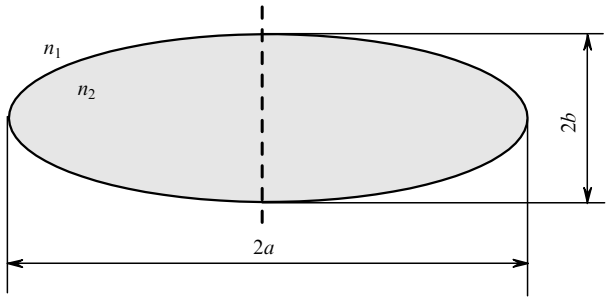

Figure 1. Schematic representation of a spheroid. The dashed line shows the symmetry axis of the spheroid.

2.1 Discrete-dipole approximation

The discrete-dipole approximation is applicable for particles whose size is comparable with the optical wavelength. In this approach, the particle of any shape is replaced by a set of point dipoles. The distance between the neighboring dipoles should be small compared to the optical wavelength. Each dipole oscillates under the action of the incident light wave as well as of the electric fields, radiated by all other dipoles of the ensemble. The dipole momentum of the dipole is

$$\boldsymbol{d}_1 = \alpha_i \boldsymbol{E}_i, \tag{1}$$

where i is the dipole number; α_i is its polarisability; $\boldsymbol{E}_i$ is the electric field strength in the point of space where the dipole is located. The electric field strength is presented as a sum

$$\boldsymbol{E}_i = \boldsymbol{E}_{\text{inc}} + \boldsymbol{E}_{\text{d}} \tag{2}$$

of the incident field $\boldsymbol{E}_{\text{inc}}$ and the field

$$\boldsymbol{E}_{\text{d}} = \sum_{j \neq i} \boldsymbol{E}_j \tag{3}$$

created in the given point of space by all other dipoles of the ensemble. The expression for the electric field strength $\boldsymbol{E}_j$, induced by the jth dipole at the point where the ith dipole is located, can be written in the form

$$\boldsymbol{E}_j = \frac{\exp[-\mathrm{i}(kr_{ij} - \omega t)]}{r_{ij}} \left\{ \frac{1 + \mathrm{i}kr_{ij}}{r_{ij}^2} \left[\frac{3(\boldsymbol{d}_j \boldsymbol{r}_{ij})\boldsymbol{r}_{ij}}{r_{ij}^2} - \boldsymbol{d}_j \right] - k^2 \left[\frac{(\boldsymbol{d}_j \boldsymbol{r}_{ij})\boldsymbol{r}_{ij}}{r_{ij}^2} - \boldsymbol{d}_j \right] \right\}. \tag{4}$$

Here r_{ij} is vector directed from the jth dipole to the ith one; k is the wave number; ω is the optical wave frequency; and t is the time.

The system of linear coupled equations (1)–(4) consists of equations, whose number is equal to the number of dipoles in the ensemble and, in principle, it enables one to find the dipole momentum for each individual dipole of the ensemble. In other words, one can find a self-consistent radiation field of the dipole ensemble, arising under the action of the incident optical wave. Unfortunately, the numerical solution of the equations becomes unstable, if the number of the dipoles becomes too large. As noted in [18], at present the calculations can not be performed for the ensembles in which the total number of dipoles exceeds 10^6. This imposes limitations for the size of the particles, which can be considered within the framework of the DDA. In practice this method has troubles in calculations of light scattering by particles with the size parameter higher than 100.

To calculate the light scattering with the DDA technique, we used the ADDA software (Amsterdam Discrete Dipole Approximation) developed by A. Hoekstra and coworkers [19–21]. With the help of this code, we have calculated light scattering by dielectric spheroids with different sizes, refraction indices and spatial orientations. The calculations were performed by using an Intel Pentium 4 PC (1.73 GHz frequency, and 512 Mb RAM). Comparison of the results obtained with the DDA code and the Mie theory for spherical particles shows almost an ideal agreement [22]. Unfortunately, the calculation time grows rapidly as a function of the particle size. For example, it was around 50 seconds for a sphere with the relative refractive index $n = 1.05$ and the diameter 4 microns, and it was about 7 hours for a sphere of the same material with the diameter 8 microns.

2.2 Geometrical optics approximation

This approximation is valid for particles, whose size is much larger than the optical wavelength. In the geometrical optics approximation (GOA) the light illuminating the particle is presented as a set of partial rays. Each of the rays obeys the geometrical optics laws of reflection and refraction at the particle boundaries. The ray is described by a set of parameters associated usually with the plane wave, namely, by the amplitude, phase and propagation direction.

Here we use the following procedure to calculate the reflection and refraction of light. An incident ray is assumed to be unpolarised. We calculate intensities of reflected and refracted rays by using Snell's law and Fresnel formulae. Then we change the reflected and refracted rays by unpolarised rays of the same intensities. This gives a possibility to describe the reflection and refraction events

in terms of the light intensity only without introducing such parameters as amplitudes of the orthogonal components of the field and phase shift between them. This approach can be called the scalar approximation or the approximation of unpolarised rays. In this approach the energy reflection coefficient is defined by the expression (see, for example, [23])

$$R = \frac{1}{2}\left[\frac{\sin^2(\alpha-\beta)}{\sin^2(\alpha+\beta)} + \frac{\tan^2(\alpha-\beta)}{\tan^2(\alpha+\beta)}\right], \tag{5}$$

where α is the angle of incidence of the ray at the interface between two media; β is the angle of refraction. The energy transmission coefficient has the form

$$T = (1-R)\frac{\cos\alpha}{\cos\beta}. \tag{6}$$

The factor $\cos\alpha/\cos\beta$ in equation (6) takes into account the change in the optical beam cross-section area due to refraction.

One of the partial rays is shown in Fig. 2a. It impinges onto the particle surface at an angle α. In the point M_1 at the particle surface the incident ray splits into reflected and refracted rays. The refracted ray reaches the particle surface in the point M_2, where it experiences reflection and refraction of light. Then the described process goes on. As a result, the incident ray energy is distributed among the rays emerging from the particle. The corresponding energy distribution can be calculated. The calculation is performed independently for each incident partial ray. Then we sum the scattered waves to obtain the resulting scattering diagram. The summation can be performed for the rays with complex amplitudes (coherent case) or for the partial rays with intensities (incoherent case) [24]. In our calculations, the total number of partial rays was 10^6 and 15 internal reflections inside the particle were taken into account. In many cases these values can be essentially decreased without the loss of the calculation accuracy.

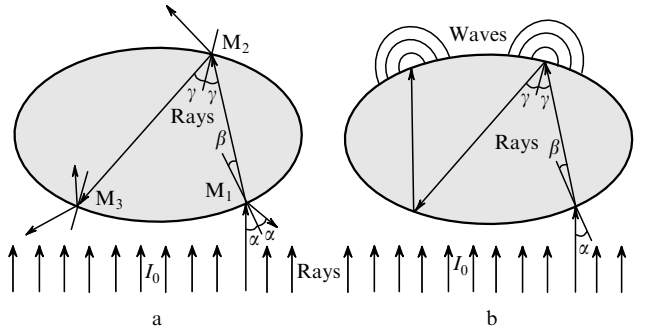

Figure 2. Schematics of light scattering in geometrical optics (a) and ray-wave (b) approximations.

To estimate the accuracy of the GOA, we calculated the angular distribution of the intensity of light scattered by spherical particles. The results were compared with data, obtained by using the Mie theory and DDA [22]. Analysis of the scattering pattern in the far-field zone, calculated for a sphere of 5 microns in diameter and the relative refraction index $n = 1.05$, shows that the calculation accuracy of the GOA is significantly lower than that of the DDA. We believe that one of the reasons is that the GOA does not take into account the diffraction of rays emerging from the particle.

2.3 Ray-wave approximation

Diffraction of light emerging from the particle can be described with the help of the Huygens–Fresnel principle and Kirchhoff's diffraction integral. To do this, we consider an element of the particle surface, from which the optical rays come outside, as the origin of the elementary spherical waves. The incident light and the light inside the particle are presented by a set of rays, as before. We refer to this approach, which combines the elements of ray and wave optics, as the ray-wave approximation (RWA).

Let us present the complex amplitude of the field $E(\mathrm{P})$ in the observation point P in the form of an integral over the particle surface S (Kirchhoff integral – see, for example [23]):

$$E(\mathrm{P}) = \frac{1}{4\pi}\oint_S \left(G\frac{\partial E}{\partial v} - E\frac{\partial G}{\partial v}\right)\mathrm{d}S. \tag{7}$$

Here E is the field amplitude at the particle surface; $\partial/\partial v$ is a derivative taken along the normal to the particle surface;

$$G = \frac{\exp(-\mathrm{i}k\rho)}{\rho} \tag{8}$$

is the Green function; ρ is the distance between the particle surface element $\mathrm{d}S$ and the observation point P. The field amplitude at the particle surface is presented as the sum of amplitudes of partial waves (rays):

$$E = \sum_j E_j(\mathrm{M})\exp(-\mathrm{i}\boldsymbol{k}_j\boldsymbol{r}). \tag{9}$$

By substituting equations (9) and (8) into (7), we obtain

$$E(\mathrm{P}) = \frac{\mathrm{i}}{\lambda}\oint_S E(\mathrm{M})\frac{\exp(-\mathrm{i}k\rho)}{\rho}\mathrm{d}S, \tag{10}$$

$$E(\mathrm{M}) = \sum_j E_j(\mathrm{M})K_j, \tag{11}$$

$$K_j = \frac{1}{2}\boldsymbol{\nu}\boldsymbol{\kappa}_j + \frac{1}{2}\boldsymbol{\nu}\boldsymbol{\rho}_0, \tag{12}$$

where $\boldsymbol{\nu}$ is the unit vector of the external normal to the particle surface in the point M; $\boldsymbol{\kappa}_j$ is the unit vector directed along the jth ray; $\boldsymbol{\rho}_0$ is the unit vector directed from point M to point P (Fig. 3). The values $E_j(\mathrm{M})$ can be calculated with the help of expressions presented in [24]. In this paper Fresnel formulae are presented in the form suitable for

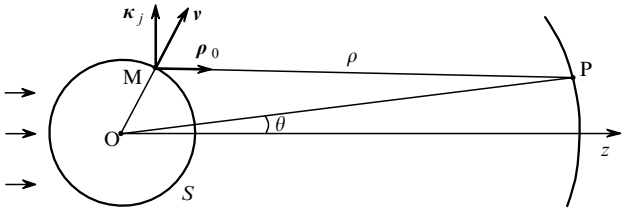

Figure 3. Schematics of vector directions for calculating Kirchhoff's diffraction integral.

solving our problem, in which we need to introduce many local coordinate systems.

Expression (7) for Kirchhoff's diffraction integral is written in the usual scalar form, which means the change of all the rays emerging from the particle, by the polarised rays with equal polarisations.

The calculation result is the relative scattering intensity, or the scattering phase function, defined as follows:

$$f(\theta,\varphi)=\frac{I(\theta,\varphi)}{I_0}\frac{4\pi R_0^2}{\sigma}, \tag{13}$$

where I is the scattered light intensity; θ is the scattering angle; φ is the angle, which determines orientation of the scattering plane with respect to the plane of the incident light beam and the spheroid axis of symmetry; I_0 is the incident light intensity; R_0 is the observation sphere radius; σ is the scattering cross section, which is defined as a ratio of the incident beam power P_0 and its intensity I_0. For a spheroidal particle

$$\sigma=\pi aA, \tag{14}$$

$A^2=a^2\cos^2\theta_0+b^2\sin^2\theta_0$; a and b are the spheroid semiaxes; θ_0 is the tilt angle of the spheroid axis of symmetry relative to the incident beam axis (Fig. 4).

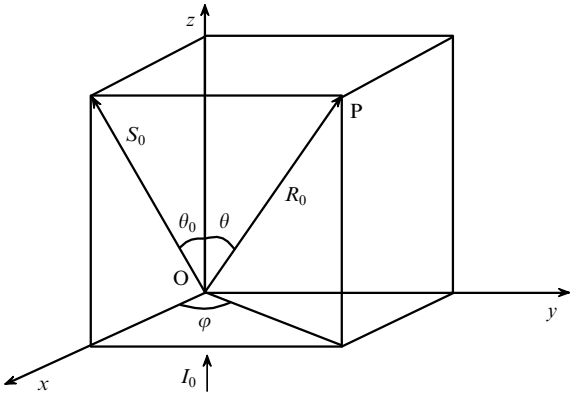

Figure 4. Laboratory system of coordinates xyz for calculating the light scattering by a particle: O – the origin of coordinates and centre of the spheroid; S_0 – spheroid axis of symmetry; θ_0 – tilt angle of the spheroid symmetry axis relative to the incident optical beam direction; θ and φ – angular coordinates of the observation point P.

To control the calculation accuracy, we used the integral, defined by the equation

$$\frac{P}{P_0}=\frac{1}{4\pi}\int_0^{2\pi}\mathrm{d}\varphi\int_0^{\pi}f(\theta,\varphi)\sin\theta\mathrm{d}\theta, \tag{15}$$

where P is total power of the scattered light. In our calculations, the ratio P/P_0 was close to unity (the difference being below 4 %).

As a simple test problem, we have considered the scattering of a plane light wave by a dielectric cylinder, assuming that the incident optical wave propagates along the cylinder axis of symmetry [22]. In this case the scattering pattern can be calculated analytically by expressions (10)–(12) and is very close to the diffraction pattern of light at a round aperture (Airy pattern). This was confirmed by the calculation, performed with the help of the DDA. Of course, such scattering pattern could not be obtained within the framework of the GOA, consequently, the RWA has an obvious advantage compared to the GOA.

Note, that earlier a somewhat similar approach for calculating the light scattering by a spheroid was proposed in papers [25–27] and was called the physical optics approximation.

3. Results and discussion

As noted above, the description of light scattering by erythrocytes located in blood plasma is an important applied problem. Therefore, in our calculations, we supposed the size parameters and relative refractive index of spheroids to be close to the parameters of erythrocytes in blood. Note that a normal erythrocyte can be regarded as a biconcave disc with a diameter of about 6.5 μm, minimum and maximum thicknesses of about 1.0 and 2.3 μm, respectively. The refractive index of an erythrocyte substance relative to blood plasma is ~ 1.05. The optical radiation wavelength is supposed to be equal to 0.633 μm which corresponds to the wavelength of a He–Ne laser. Note that the light wavelength is an order of magnitude less than the linear size of an erythrocyte.

We have calculated the light scattering by spheroids for different sizes and relative refractive indices of spheroids, as well as for different orientations of the spheroid and the scattering plane. Calculations are performed for the far-field zone ($R_0 = 100$ μm) by using different approximations: DDA, RWA and GOA. The results are shown in Figs 5–8. For better clearness, in all illustrations, the orientation of the spheroid symmetry axis (dashed line) is shown in relation to the direction of the incident beam (arrows). The calculation time when using the RWA was usually around 15–20 min.

One can see from Figs 5 and 6 that the RWA describes the light scattering by a spheroid much more precisely than the GOA. Since the incident ray is parallel to the particle symmetry axis, the scattering diagram does not depend on the angle φ, defining the orientation of the scattering plane.

One can see from Figs 7a, b that the angle coordinates and the widths of the maxima and minima of the light

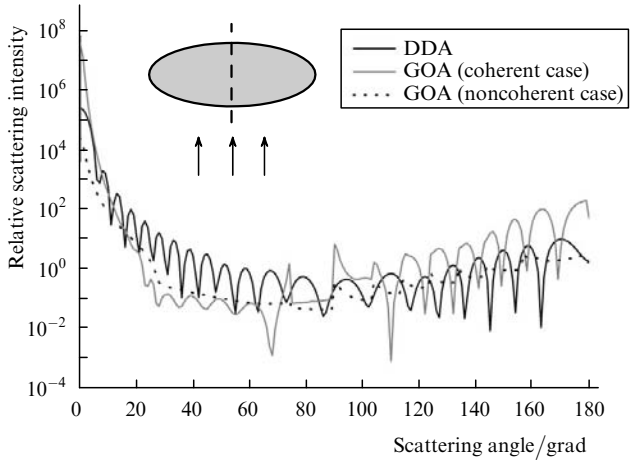

Figure 5. Diagrams of laser radiation scattering by a spheroid upon its illumination along the symmetry axis ($\theta_0 = 0$) obtained by using the DDA and GOA (both coherent and noncoherent cases). The spheroid semiaxes $a = 4$ μm and $b = 1$ μm, the relative refractive index $n = 1.05$.

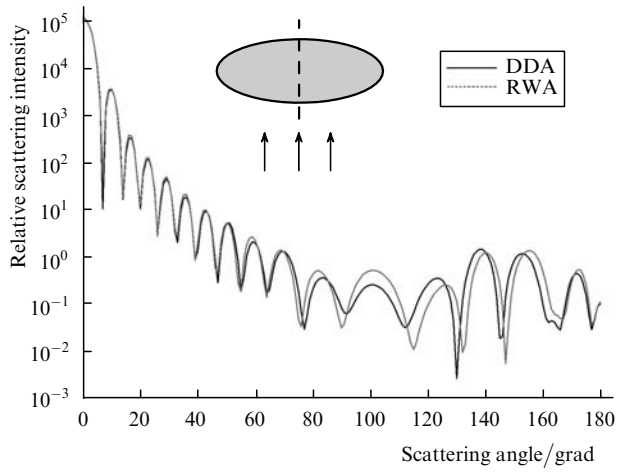

Figure 6. Diagrams of laser radiation scattering by a spheroid upon its illumination along the symmetry axis ($\theta_0 = 0$) obtained by using the DDA and RWA. The spheroid semiaxes $a = 3.25$ μm and $b = 1.15$ μm, the relative refractive index $n = 1.05$.

intensity change depending on the orientation of the scattering plane, especially at low scattering angels. This is due to the difference in transverse particle sizes at different scattering planes. Curves shown in Fig. 7a relate to the scattering plane in which the lateral size of the particle is small. Curves in Fig. 7b, conversely, relate to the scattering plane in which the lateral size of the particle is large. As is well known from the diffraction theory, the angular distribution of the light intensity in the far-field zone is defined by the angular radiation spectrum. The width of the angular spectrum $\Delta\theta$ is related to the lateral size d of the scattering particle in the scattering plane: $\Delta\theta \approx \lambda/d$. Therefore, one can expect that the larger this size d the smaller the width of the angular scattering spectrum. Data presented in Fig. 7 confirm this conclusion.

Data shown in Fig. 7c relate to the case in which the scattering plane ($x = 0$) is perpendicular to the system symmetry plane ($y = 0$). One can see that the angular distributions of intensities are symmetrical relative to the incident beam direction. This can be explained by the fact that in this case the cross section of the spheroid in the scattering plane is represented by an ellipse with the large semiaxis perpendicular to the incident beam.

Data shown in Fig. 7d relate to the case in which the scattering plane coincides with the symmetry plane of the system ($y = 0$). One can see that the angular distributions of the intensities are nonsymmetrical relative to the incident beam direction. This can be explained by the fact that in this case the cross section of the spheroid in the scattering plane is represented by an ellipse with the large semiaxis located at an angle of 45° relative to the incident beam.

In the calculations presented above, the scattering particle was supposed to be optically soft, i.e. the relative refractive index $n = 1.05$. This corresponds to the case of light scattering by an erythrocyte in blood plasma. It is interesting to know how the scattering diagram is transformed with increasing the optical density of the particle. As an example, a scattering diagram for a spheroid with relative

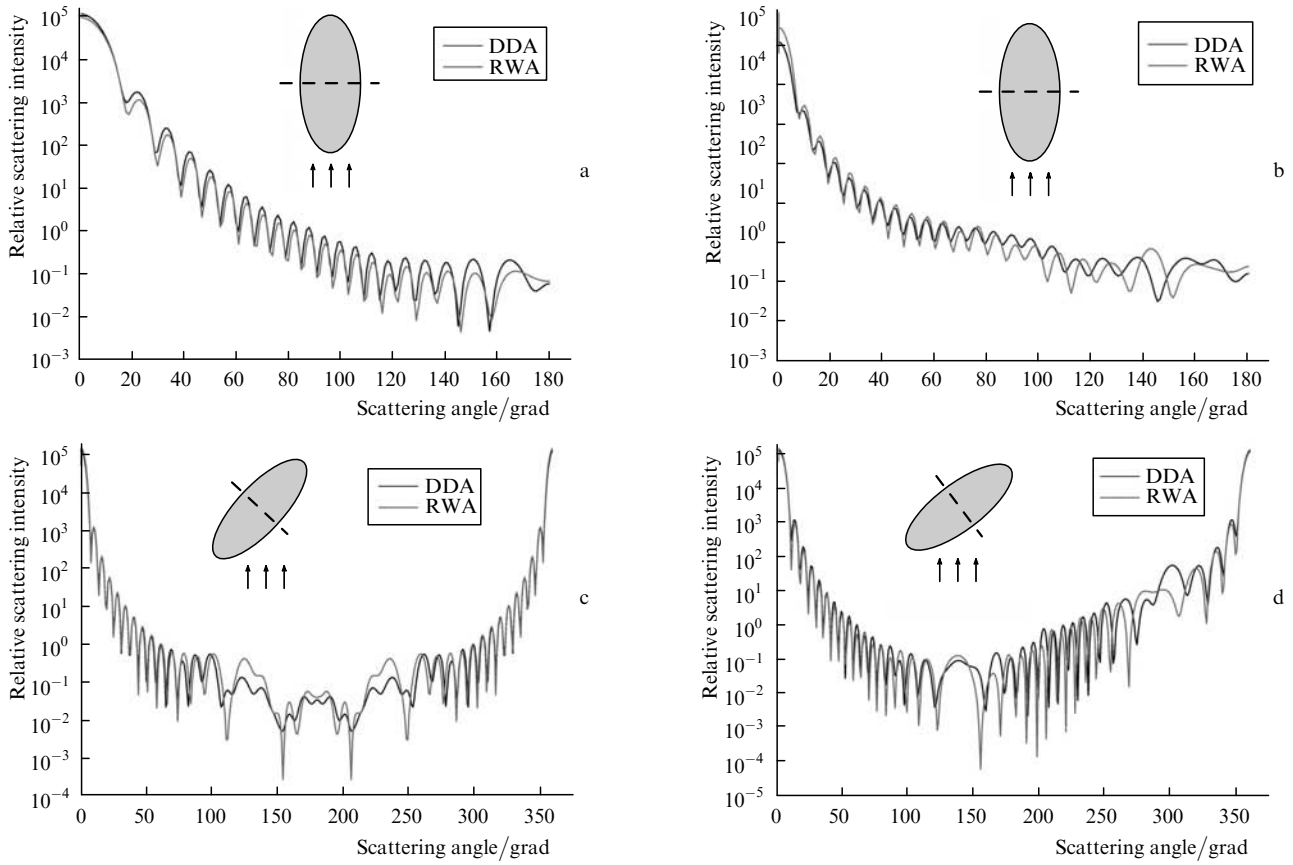

Figure 7. Diagrams of laser radiation scattering by a spheroid obtained by using the DDA and RWA at $\theta_0 = 90°$, $\varphi = 0$ (a), $\theta_0 = 90°$, $\varphi = 90°$ (b), $\theta_0 = 45°$, $\varphi = 90°$ (c) and $\theta_0 = 45°$, $\varphi = 0$ (d). The spheroid semiaxes $a = 3.25$ μm and $b = 1.15$ μm, the relative refractive index $n = 1.05$.

refractive index $n = 1.33$ is shown in Fig. 8. One can see that in this case the curves calculated with the help of the RWA and DDA match well. The calculation time in the case of the RWA remains the same ($\sim$ 15 min) while in the case of the DDA it significantly increases ($\sim$ 170 min). For a particle with the same shape and relative refractive index $n = 1.5$, the calculation by the DDA method requires more than 1 day on a conventional personal computer.

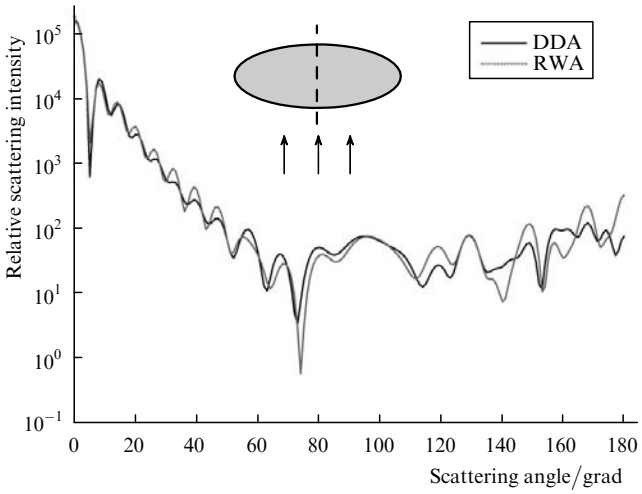

Figure 8. Diagrams of laser radiation scattering by a spheroid upon its illumination along the symmetry axis ($\theta_0 = 0$) obtained by using the DDA and RWA. The spheroid semiaxes $a = 3.25$ μm and $b = 1.15$ μm, the relative refractive index $n = 1.33$.

With increasing the particle refractive index, the visibility of the interference maxima and minima in the scattering pattern decreases, while the intensity of scattering decreases slower at large scattering angels, i.e. the angular spectrum of scattering becomes wider (compare Figs 6 and 8) and the general scattering pattern becomes 'smoothed'.

The qualitative characteristics of the angular distribution of intensities of the scattered light in the forward half-space, especially at small scattering angles, conform to the general principles of the diffraction theory. Reflection of the incident light plays a decisive role for the back half-space.

One can see from Figs 6–8 that the calculation results obtained by using the RWA and DDA methods agree well.

We have also considered the problem of the effect of the longitudinal size of the spheroid on the scattering pattern. The scattering diagrams for the case of the spheroids with equal cross sections, but different sizes in the direction of the incident beam were constructed. The comparison of these diagrams allowed us to conclude that the longitudinal size of the particle influences the visibility of the interference maxima and minima in the scattering pattern, however, it does not influence their position in the region of small scattering angles ($\theta \leqslant 30^\circ$), namely, the contrast of the scattering pattern decreases with increasing the spheroid size in the direction of the laser beam.

4. Conclusions

Thus in this work, a theoretical model is developed and a numerical algorithm is proposed for calculating the light scattering by transparent dielectric particles with the size parameter highly exceeding the light wavelength. The results of calculations show that the presented algorithm is comparable in precision with such a method as the DDA, however, it significantly exceeds the latter in the calculation rate for particles with the size parameter higher than 100. For example, for particles with the size parameter 85 and the relative refractive index 1.33, the calculation time for the RWA was about 20 min, while for the DDA – about three hours. This algorithm is promising for fast calculations of light scattering diagrams by such particles as erythrocytes and their aggregates.

Acknowledgements. Authors thank M. Yurkin for consultations on implementing the ADDA code. This work was partially supported by the Russian Foundation for Basic Research (Grant Nos 06-02-17015-a and 07-02-01000-a).

References

1. Yaroslavskaya A.N., Priezzhev A.V., Rodrigues J., Yaroslavsky I.V., Battarbee H., in *Handbook of Optical Biomedical Diagnostics*. Ed. by V.V. Tuchin (Bellingham: SPIE Press, 2002) Chapt. 2, p. 169.
2. Lopatin V.N., Priezzhev A.V., Aponasenko A.D., Shepelevich N.V., Lopatin V.V., Pozhlenkova P.V., Prostakova I.V. *Methody svetorasseyaniya v analize dispersnykh biologicheskikh sred* (Light Scattering Methods in the Analysis of Aqueous Disperse Biological Media) (Moscow: Fizmatlit, 2004).
3. Turcu I. *Appl. Opt*., **45** (4), 639 (2006).
4. Maltsev V.P. *Rev. Sci. Instr*., **71**, 243 (2000).
5. Rinkevichus B.S. *Lazernaya diagnostika potokov* (Laser Diagnostics of Flows) (Moscow: Moscow Power Engineering Institute Publ., 1990).
6. Asano S., Yamamoto G. *Appl. Opt*., **14**, 29 (1975).
7. Asano S. *Appl. Opt*., **18**, 712 (1979).
8. Mishchenko M.I., Hovenier J.W., Travis L.D. *Light Scattering by Nonspherical Particles* (London: Acad. Press, 2000).
9. Voshchinnikov N.V., Farafonov V.G. *Meas. Sci. Technol*., **13**, 249 (2002).
10. Farafonov V.G., Il'in V.B., Henning T. *J. Quant. Spectr. Rad. Transfer*, **63**, 205 (1999).
11. Farafonov V.G., Il'in V.B. *Opt. Spektrosk*., **100** (3), 484 (2006).
12. Shepelevich N.V., Prostakova I.V., Lopatin V.N. *J. Quant. Spectr. Rad. Transfer*, **63**, 353 (1999).
13. Lock J.A. *Appl. Opt*., **35** (3), 500 (1996).
14. Lock J.A. *Appl. Opt*., **35** (3), 515 (1996).
15. Rysakov W., Ston M. *J. Quant. Spectr. Rad. Transfer*, **69**, 651 (2001).
16. Rysakov V. *J. Quant. Spectr. Rad. Transfer*, **87**, 261 (2004).
17. Han Y.P., Mees L., Ren K.F., Gouesbet G., Wu. S.Z., Grehan G. *Opt. Commun*., **210**, 1 (2002).
18. Kokhanovsky A. *Light Scattering Media Optics* (Chichester: Springer – Praxis Publ., 2004).
19. Yurkin M.A., Maltsev V.P., Hoekstra A.G. *J. Quant. Spectr. Rad. Transfer*, **106**, 546 (2007).
20. Yurkin M.A., Hoekstra A.G. *J. Quant. Spectr. Rad. Transfer*, **106**, 558 (2007).
21. Penttila A., Zubko E., Lumme K., Muinonen K., Yurkin M.A., Draine B.T., Rahola J., Hoekstra A.G., Shkuratov Y. *J. Quant. Spectr. Rad. Transfer*, **106**, 417 (2007).
22. Lugovtsov A.E., Priezzhev A.V., Nikitin S.Yu. *Proc. SPIE Int. Soc. Opt. Eng*., **6534**, 65340N (2007).
23. Akhmanov S.A., Nikitin S.Yu. *Physical Optics* (Oxford: Clarendon Press, 1997; Moscow: Moscow University Press, 1998).
24. Lugovtsov A.E., Priezzhev A.V., Nikitin S.Yu. *J. Quant. Spectr. Rad. Transfer*, **106**, 285 (2007).
25. Ravey J.-C., Mazeron P. *J. Opt. (Paris)*, **13** (5), 273 (1982).
26. Ravey J.-C., Mazeron P. *J. Opt. (Paris)*, **14** (1), 29 (1982).
27. Mazeron P., Muller S. *Appl. Opt*., **35**, 3726 (1996).